

# Acid–base properties of 3,5-dimethyl-1,7-diphenyl derivative of bis-pyrazolopyridine in non-aqueous solutions

Danuta Grabka<sup>a,\*</sup>, Wojciech Boszczyk<sup>a</sup>, Yuriy Stepanenko<sup>c</sup>, Stanisław Styrz<sup>a</sup>,  
Marta Kubik<sup>a</sup>, Krystyna Rotkiewicz<sup>a,b</sup>, Andrzej Danel<sup>d</sup>

<sup>a</sup> Świętokrzyska Academy, Institute of Chemistry, Chęcińska 5, PL-25-020 Kielce, Poland

<sup>b</sup> Institute of Physical Chemistry, Polish Academy of Sciences, Kasprzaka 44, PL-01-224 Warsaw, Poland

<sup>c</sup> Laser Center at Institute of Physical Chemistry, Polish Academy of Sciences, Kasprzaka 44, PL-01-224 Warsaw, Poland

<sup>d</sup> Department of Chemistry, University of Agriculture, Al. Mickiewicza 24/28, PL-30-059 Cracow, Poland

Received 29 November 2004; received in revised form 27 September 2005; accepted 28 September 2005

Available online 9 November 2005

## Abstract

Acid–base properties of 3,5-dimethyl-1,7-diphenyl-bis-pyrazolo-[3,4-b;4',3'-e]-pyridine (BPP) in the ground state and in the first excited singlet state were investigated in non-aqueous solutions. Absorption and stationary fluorescence spectroscopy, supersonic jet spectroscopy as well as the calculations of effective valence potentials were applied as methods. The sequence of the protonation of BPP nitrogen atoms in solutions and the formation of complexes with water in molecular beams were discussed.

© 2005 Elsevier B.V. All rights reserved.

**Keywords:** Bis-pyrazolopyridines; Acid–base properties; Fluorescence; Supersonic jet

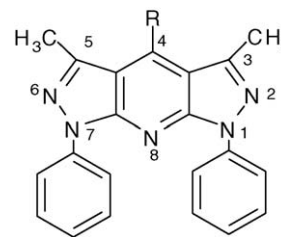
## 1. Introduction

3,5-Dimethyl-1,7-diphenyl-bis-pyrazolo-[3,4-b;4',3'-e]-pyridine (BPP) is the parent compound for numerous derivatives with valuable properties in the aspect of recognition and application.

The derivatives of BPP with (4'-N,N-alkylaminophenyl) in position 4 show a low lying highly dipolar charge-separated excited state, and are therefore promising candidates for efficient non-linear optical (NLO) materials.

Derivatives with various other substituents in position 4 showing intense fluorescence can be used as fluorescence standards and have found application as blue-green organic light-emitting diodes [1,2]. Some of BPP derivatives show biological activity and are considered as medicines [3].

The acid–base properties of four derivatives: DMA-DMPP, H-DMPP, NO<sub>2</sub>-DMPP and CH<sub>3</sub>O-DMPP (see Formulae 1) were investigated previously [4,5].



The donor–acceptor molecule, DMA-DMPP, has three different possible protonation centers and undergoes the protonation in step-by-step processes. The amino group is protonated as the first one in the ground as well as in the excited state. The question arises which nitrogen atom in heterocyclic subunit is protonated as the next one. The results of semi-empirical calculations [4] hinted at the protonation of pyridine nitrogen, but the prevention from such protonation due to steric hindrance of phenyls 1 and 7 was also mentioned [6]. On the other hand, the effective valence electron potentials hint to protonation of pyrazolic nitrogen in the molecule already protonated on the amino group [5]. The basic properties of N,N-dimethylamino group in DMA-DMPP practically do not change in the first excited singlet state, S<sub>1</sub>. The basicity of the nitrogen protonated in the second step increases

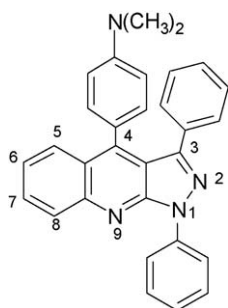
\* Corresponding author. Tel.: +48413497051; fax: +48413614942.

E-mail address: [danuta.grabka@pu.kielce.pl](mailto:danuta.grabka@pu.kielce.pl) (D. Grabka).

remarkably in the  $S_1$  state. The protonation occurs much easier in acetonitrile solutions than in ethanolic ones.

The three other studied derivatives H-,  $\text{NO}_2$ - and  $\text{CH}_3\text{O}$ -DMPP, undergo protonation as it is in the case of the second step of DMA-DMPP.

In the present paper, we describe the results of the investigations of BPP acid–base properties in the ground state and in the  $S_1$  state, which should be helpful in deeper understanding of the protolytic processes in the four compounds described in [4]. The comparison of the behaviour of BPP with that of the above mentioned compounds and first of all with that of DMA-DPPQ [7] (Formula 2) led to the assignment of protonation sequence in heterocyclic system.



The investigations were performed for non-aqueous solutions, i.e. in acetonitrile and ethanol as solvents, because of sparingly small solubility of BPP in water. Additionally, the clusters of BPP with water molecule were studied in a supersonic jet.

## 2. Materials, experimental and computation methods

BPP was synthesized and purified according to Brack [8]. The solvents and  $\text{HClO}_4$  (72% w/w) were of the highest available quality and checked for impurities by means of absorption and fluorescence spectroscopy. Absorption spectra were measured with a Specord M 500 spectrophotometer. Fluorescence spectra and fluorescence excitation spectra were measured with a Kontron SFM 25 spectrofluorimeter.

All spectra of jet-cooled BPP were obtained with a home-built jet spectrometer. The sample was heated to  $190^\circ\text{C}$  and injected through a  $500\ \mu\text{m}$  pulsed nozzle (General Valve Series 9) into the vacuum chamber evacuated by a turbomolecular pump (Leybold Turbovac 600C). Helium was used as a carrier gas. A home-built dye laser with spectral width of  $<0.2\ \text{cm}^{-1}$ , pumped by the 3rd harmonic of a Nd:YAG laser (Surelite I-10) was used for fluorescence excitation. Total fluorescence was collected by a toroidal mirror and imaged onto a cooled photomultiplier (Hamamatsu R). The signal from the photomultiplier was digitized by a digital oscilloscope (Le Croy 9310) and stored in a personal computer. Molecular clusters of BPP and water were formed in the jet by passing the carrier gas through the reservoir with the solvent. The amount of the solvent added into the carrier gas and the stoichiometry of the complexes formed were controlled by changing the reservoir temperature.

To estimate the reactivities of different aza-atoms, we calculated the Spanget-Larsen's indexes of reactivity [2,9–11], called

effective potential energies of valence electrons ( $\mu^A$  – for  $\mu$  orbital of A atom) or effective valence potentials. These potentials can be defined in terms of atomic charges and interactions between atoms:

$$W_\mu^A = W_\mu^A(q_A) + \sum_{B \neq A} W_\mu^A(q_B) \quad (1)$$

$$W_\mu^A(q_A) = -(a + bq_A)^{3/2} \quad (2)$$

$$W_\mu^A(q_B) = \gamma_{AB}(q_B - Z'_B) \quad (3)$$

where  $q_A$  and  $q_B$  are total electron populations on A and B atoms. The  $\gamma_{AB}$  is the Coulomb integral representing repulsing interactions between valence electrons of A and B atoms. The  $a$  and  $b$  constants were derived from the dependence of ionization potentials on cation and anion charges.  $Z'_B$  denotes the number of valence electrons in the neutral atom B.

The ability of aza-atoms to attach a proton can be estimated from effective potentials calculated in this way. Higher positive values of  $W_\mu^A$  correspond to a higher basicity of the A atom and to more nucleophilic nature of the appropriate region of the molecule. We calculated  $W_\mu^A$  values only for nitrogen atoms in the heterocyclic system because this method is not good enough to estimate the basicity of N-atoms of the amino group.

Calculations of potentials were based on molecular geometries calculated by the AM1 method and charge densities were calculated by the INDO/S method.

The molecular geometries and the values of heats of formation for protonated molecules were obtained within AM1 method.

## 3. Results

### 3.1. Stationary absorption and fluorescence spectra

The absorption spectra of BPP in acetonitrile as solvent with different amounts of  $\text{HClO}_4$  are shown in Fig. 1.

Upon increasing of acid concentration, the new long wavelength band peaking at  $26\ 300\ \text{cm}^{-1}$  appears, accompanied by the changes in the short wavelength range. The band reaches its maximal absorbance at  $[\text{HClO}_4] \cong 6 \times 10^{-2}\ \text{M}$ . Further addition of acid does not change this band, but causes some changes at the short wavelength range, up to  $4 \times 10^{-1}\ \text{M}$  of acid concentration, Fig. 1c. The isobestic points hint at the equilibrium between BPP molecule and its protonated forms.

In acidified ethanolic solutions, the changes of absorption spectra of BPP are rather small (Fig. 2).

BPP emits a strong fluorescence with the maximum at  $22\ 600\ \text{cm}^{-1}$  in acetonitrile and  $22\ 500\ \text{cm}^{-1}$  in ethanol. This band is effectively quenched by acid (Fig. 3a and b) and disappears totally when  $[\text{HClO}_4] > 1.0 \times 10^{-2}\ \text{M}$  in acetonitrile solution, Fig. 3b.

The quenching of BPP fluorescence correlates with the increase of the new long wavelength absorption band, Fig. 4. The half values of the absorbance and fluorescence are reached at similar acid concentration ( $\log [\text{HClO}_4]$  in range  $-3.0$  to  $-3.4$ ). The disappearing of the fluorescence band

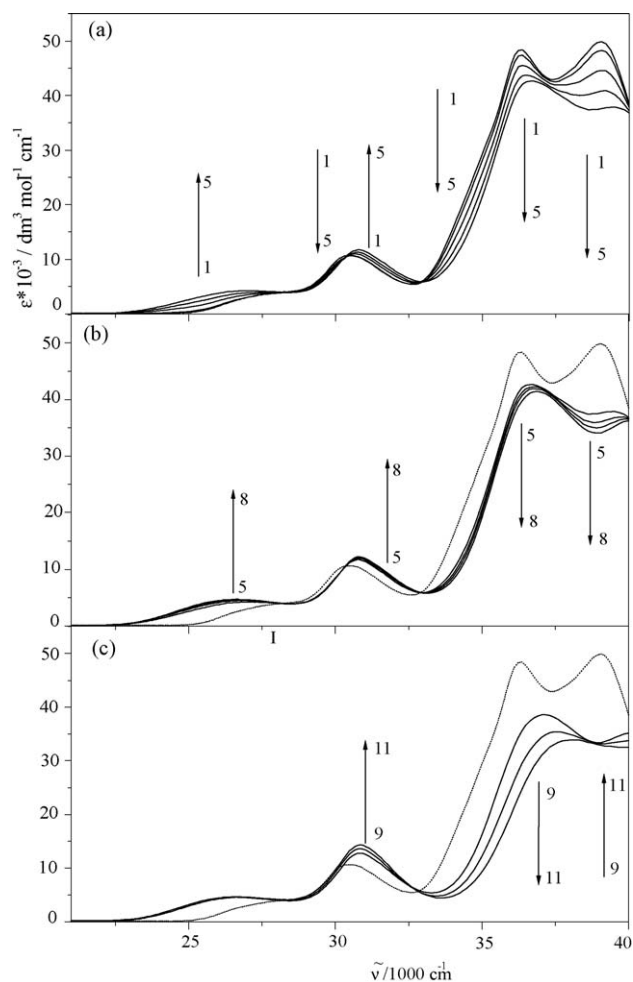


Fig. 1. Absorption spectra of BPP in acidified solutions ( $c = 2.4 \times 10^{-5}$  M) in acetonitrile. Acid concentrations: 0 M (1),  $1.1 \times 10^{-4}$  M (2),  $4.8 \times 10^{-4}$  M (3),  $1.2 \times 10^{-3}$  M (4),  $2.4 \times 10^{-3}$  M (5),  $3.8 \times 10^{-3}$  M (6),  $1.0 \times 10^{-2}$  M (7),  $3.3 \times 10^{-2}$  M (8),  $6.4 \times 10^{-2}$  M (9),  $9.7 \times 10^{-2}$  M (10),  $4.1 \times 10^{-1}$  M (11). The arrows denote the direction of absorbance changing with increasing acid concentration from 1 to 5 (a), from 5 to 8 (b) and from 9 to 11 (c). The spectrum of the unprotonated molecule (dotted line) is added for comparison to (b) and (c).

of neutral BPP ( $F_{22600}$ ) is accompanied by the creation of a new band peaking at about  $18000\text{ cm}^{-1}$  ( $F_{18000}$ ) when  $[\text{HClO}_4] > 1.4 \times 10^{-3}$  M (Fig. 3b). The band  $F_{18000}$  loses its intensity at  $[\text{HClO}_4] > 1 \times 10^{-2}$  M, Fig. 3c.

The quantum yield of the long wavelength band,  $F_{18000}$ , increases parallelly with the decreasing of the short wavelength

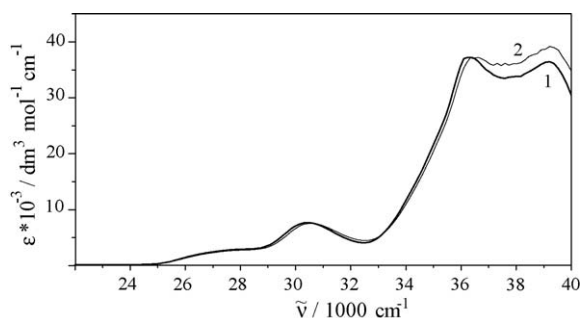


Fig. 2. Absorption spectra of BPP in ethanolic solutions ( $c = 5.0 \times 10^{-5}$  M). Acid concentration is 0 M (1) and 1.5 M (2).

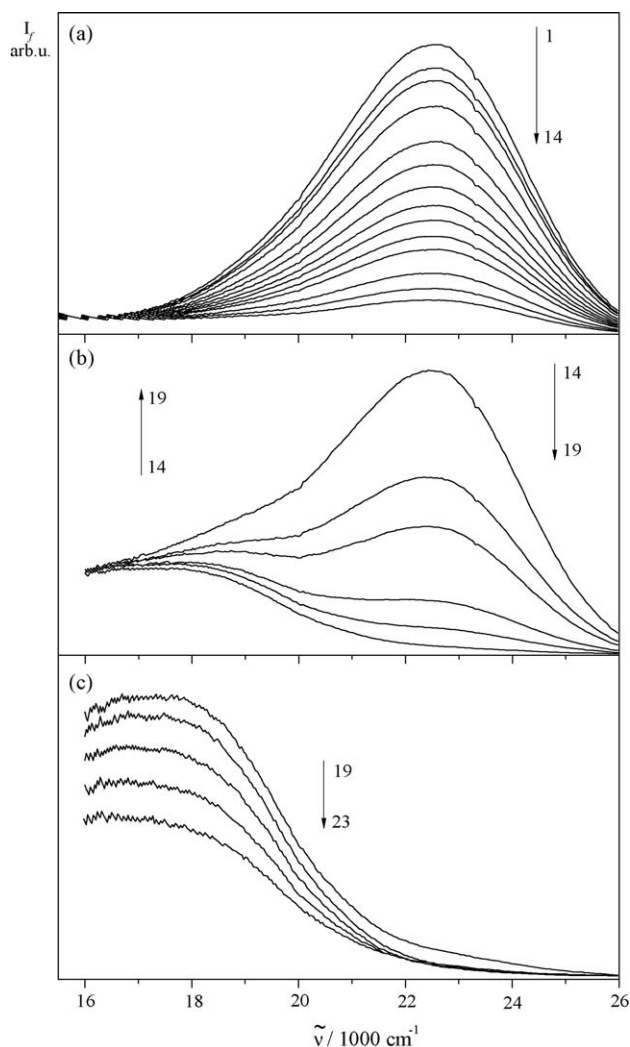


Fig. 3. Corrected fluorescence spectra ( $\tilde{\nu}_{\text{exc}} = 27322\text{ cm}^{-1}$ ) of BPP in acidified acetonitrile solutions ( $c = 2.4 \times 10^{-5}$  M). Acid concentrations: 0 M (1),  $3.6 \times 10^{-5}$  M (2),  $6.1 \times 10^{-5}$  M (3),  $1.1 \times 10^{-4}$  M (4),  $1.8 \times 10^{-4}$  M (5),  $2.5 \times 10^{-4}$  M (6),  $3.3 \times 10^{-4}$  M (7),  $4.1 \times 10^{-4}$  M (8),  $4.8 \times 10^{-4}$  M (9),  $5.8 \times 10^{-4}$  M (10),  $6.8 \times 10^{-4}$  M (11),  $9.2 \times 10^{-4}$  M (12),  $1.2 \times 10^{-3}$  M (13),  $1.4 \times 10^{-3}$  M (14),  $1.9 \times 10^{-3}$  M (15),  $2.4 \times 10^{-3}$  M (16),  $3.8 \times 10^{-3}$  M (17),  $5.7 \times 10^{-3}$  M (18),  $1.0 \times 10^{-2}$  M (19),  $2.0 \times 10^{-2}$  M (20),  $3.3 \times 10^{-2}$  M (21),  $4.6 \times 10^{-2}$  M (22),  $8.1 \times 10^{-2}$  M (23).

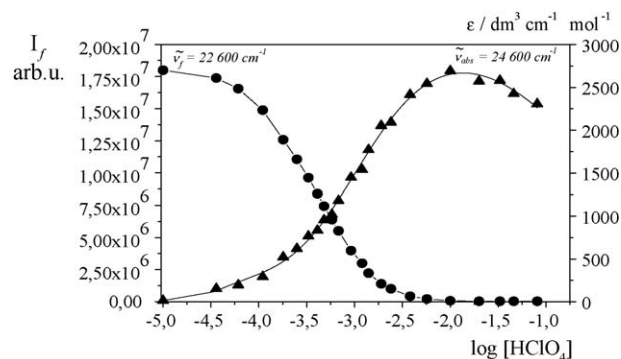


Fig. 4. The molar excitation coefficients (triangles) and fluorescence intensity (circles) of BPP in acidified acetonitrile solutions as  $\log [\text{HClO}_4]$  function.

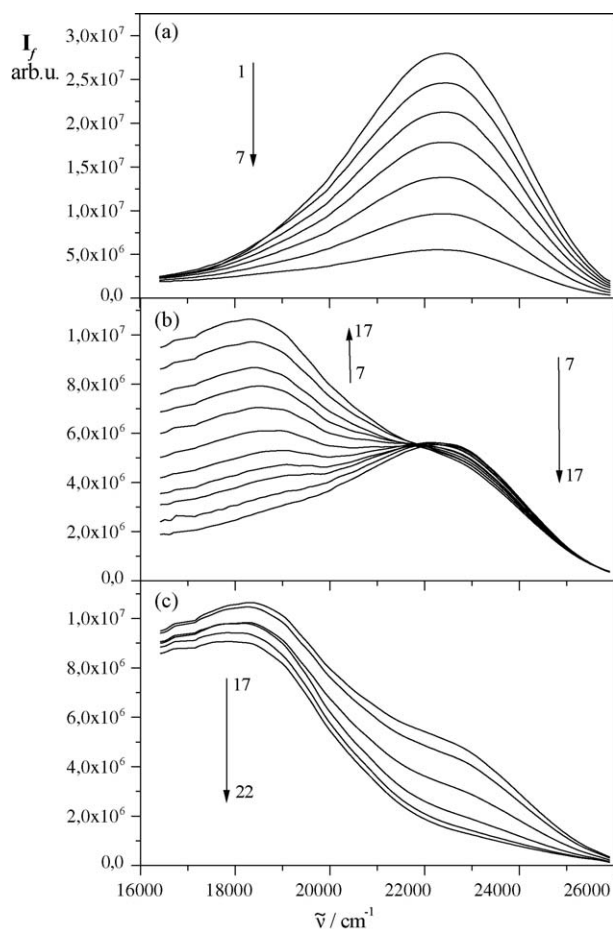


Fig. 5. Corrected fluorescence spectra of BPP ( $\tilde{\nu}_{\text{exc}} = 27322 \text{ cm}^{-1}$ ) in acidified ethanolic solutions ( $c = 5.0 \times 10^{-5} \text{ M}$ ). Acid concentrations: 0 M (1),  $1.3 \times 10^{-2} \text{ M}$  (2),  $1.7 \times 10^{-2} \text{ M}$  (3),  $2.0 \times 10^{-2} \text{ M}$  (4),  $2.7 \times 10^{-2} \text{ M}$  (5),  $3.7 \times 10^{-2} \text{ M}$  (6),  $6.0 \times 10^{-2} \text{ M}$  (7),  $8.0 \times 10^{-2} \text{ M}$  (8),  $1.1 \times 10^{-1} \text{ M}$  (9),  $1.4 \times 10^{-1} \text{ M}$  (10),  $1.7 \times 10^{-1} \text{ M}$  (11),  $2.2 \times 10^{-1} \text{ M}$  (12),  $2.6 \times 10^{-1} \text{ M}$  (13),  $3.1 \times 10^{-1} \text{ M}$  (14),  $3.5 \times 10^{-1} \text{ M}$  (15),  $4.0 \times 10^{-1} \text{ M}$  (16),  $4.5 \times 10^{-1} \text{ M}$  (17),  $5.0 \times 10^{-1} \text{ M}$  (18),  $6.1 \times 10^{-1} \text{ M}$  (19),  $9.9 \times 10^{-1} \text{ M}$  (20),  $1.3 \text{ M}$  (21),  $1.5 \text{ M}$  (22).

band  $F_{22600}$ . It reaches its maximal value when  $F_{22600}$  disappears. At the highest acid concentration under study, the quantum yield of  $F_{18000}$  decreases, most probably due to fact that the next step of the protonation occurs.

In the ethanolic solutions, the fluorescence spectra of BPP show similar changes as in the case of acetonitrile solutions upon acidifying. However, the distinctly observable changes occur when acid concentrations are much larger than in acetonitrile as solvent, i.e. at  $[\text{HClO}_4] > 1.3 \times 10^{-2} \text{ M}$ , Fig. 5a.

At  $2.7 \times 10^{-2} \text{ M} < [\text{HClO}_4] < 4.5 \times 10^{-1} \text{ M}$ , a new long wavelength band appears peaking at  $18500 \text{ cm}^{-1}$  (Fig. 5b). The quasi-isoemissive point appears at  $21900 \text{ cm}^{-1}$ . Further acidifying of ethanolic solutions causes the disappearing of the isoemissive point and a small decrease of  $F_{18500}$  band (Fig. 5c).

The fluorescence excitation spectra of BPP in acetonitrile solution (uncorrected for the lamp intensity), Fig. 6(1), as well as in ethanol, are identical for different observation wavelengths, i.e. on the short and at the long wavelength edge of the band. In acidified solutions of BPP in acetonitrile, the fluorescence exci-

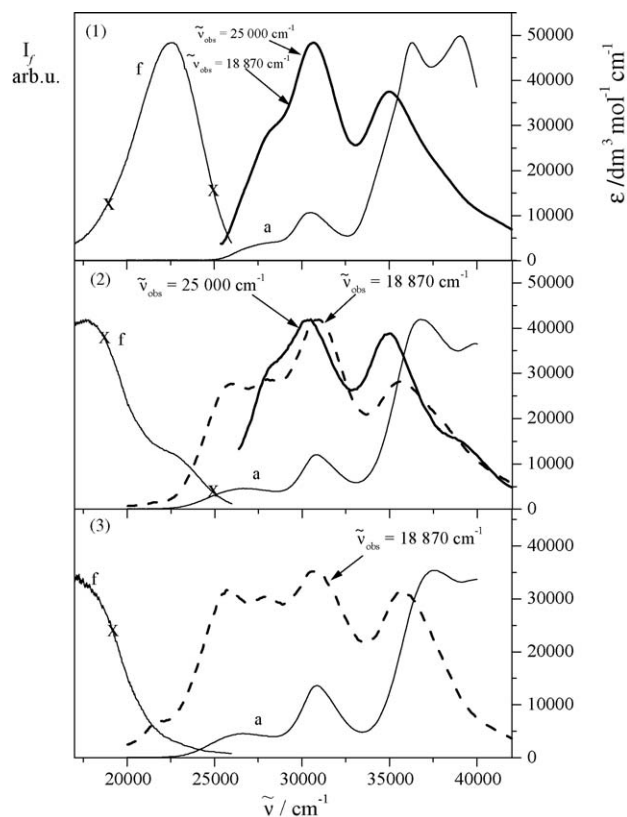


Fig. 6. The fluorescence excitation spectra of BPP (uncorrected for the lamp intensity) in acetonitrile solutions—solid bolded and dashed lines, with following acid concentrations: (1) 0 M, (2)  $5 \times 10^{-3} \text{ M}$ , (3)  $8.1 \times 10^{-1} \text{ M}$ . BPP concentration  $c = 2.4 \times 10^{-5} \text{ M}$ . For the clarity, the relevant spectra are depicted: a – absorption, f – fluorescence. The crosses on the fluorescence spectra correspond to the monitoring wave numbers.

tation spectra depend on the observation wavelength, Fig. 6(2). The spectra observed at the blue edge of the fluorescence band correspond to the absorption spectrum of a neutral molecule. Those monitored on the red edge show a new long wavelength band corresponding to the longest wavelength absorption band created in acidified solutions, Fig. 6(3).

In acidified solutions of BPP in ethanol, the fluorescence excitation spectrum of the long wavelength band is very similar to the excitation spectrum of unprotonated BPP, Fig. 7.

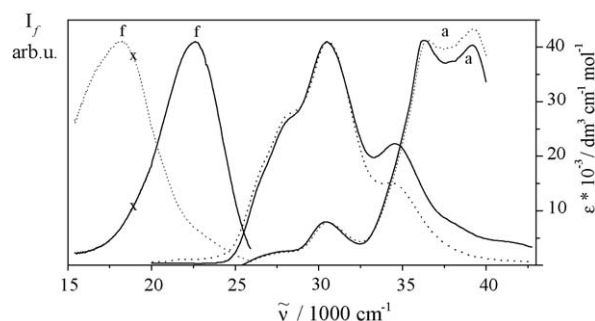


Fig. 7. The fluorescence excitation spectra of BPP,  $c = 5.0 \times 10^{-5} \text{ M}$  (uncorrected for the lamp intensity). The spectra in pure ethanol—solid lines, in acidified with  $[\text{HClO}_4] = 1.5 \text{ M}$ —dotted lines. For clarity the relevant spectra are depicted: a – absorption, f – fluorescence. The crosses on the fluorescence spectra correspond to the monitoring wave numbers.

### 3.2. Supersonic jet spectra

Fig. 8 shows a portion ( $-25$  to  $250\text{ cm}^{-1}$ ) of the fluorescence excitation spectra of jet cooled BPP molecule near the electronic origin ( $26271\text{ cm}^{-1}$ ).

The spectrum consists of the strong origin band and readily noticeable molecular progression built on this transition. Frequencies of the most intense bands are shown on the Fig. 8 and tabulated in the Table 1.

On the blue side of the BPP electronic origin, many low frequency transitions appear. There are only three fundamental low frequency modes in the electronically excited BPP molecule ( $30$ ,  $41$ ,  $67\text{ cm}^{-1}$ ) detected in the spectrum of Fig. 8. These modes form long progressions, e.g. up to five members in the case of the  $30\text{ cm}^{-1}$  vibration. Such a long progression could be treated as an evidence of a significant change of the geometry along the corresponding vibrational coordinate due to the  $S_1 \leftarrow S_0$  electronic excitation. In the region  $>250\text{ cm}^{-1}$  (inset in Fig. 8) vibronic structure is not dense, transitions are very weak and broad.

Fig. 9 shows the changes in the fluorescence excitation spectrum of BPP ( $-200$  to  $25\text{ cm}^{-1}$ ) when  $\text{H}_2\text{O}$  vapour is added. Assignments of the coordination number of the complex were made on the base of the dependence of the spectra on  $\text{H}_2\text{O}$  vapour pressure. All vibronic peaks appeared already in the presence of the lowest applied water pressure ( $0.37\text{ kPa}$ ), and simultaneously increased with increasing pressure of water, as shown in Fig. 9. Consequently, we assign these new features to 1:1 complex, BPP: $\text{H}_2\text{O}$ .

The electronic origin of the 1:1 complex is red-shifted by  $185\text{ cm}^{-1}$  with respect to the bare BPP molecule. The spectrum of the cluster demonstrates the activity of the low frequency mode ( $17\text{ cm}^{-1}$ ), seen as a very long progression of 11 quanta.

### 3.3. Calculations

The results of calculations of effective potential energies of valence electrons are collected in Table 2.

Table 1

Fundamental frequencies of the BPP and its combinations

Relative frequency, $\text{cm}^{-1}$	Assignment
0	
30	$A_0^1$
41	$B_0^1$
61	$A_0^2$
67	$C_0^1$
72	$A_0^1 B_0^1$
83	$B_0^2$
90	$A_0^3$
98	$A_0^1 C_0^1$
102	$A_0^2 B_0^1$
109	$B_0^1 C_0^1$
113	$A_0^1 B_0^2$
120	$A_0^4$
128	$A_0^2 C_0^1$
132	$A_0^3 B_0^1$
135	$C_0^2$
139	$A_0^1 B_0^1 C_0^1$
143	$A_0^2 B_0^2$
149	$A_0^5$
158	$A_0^3 C_0^1$
165	$A_0^1 C_0^2$
168	$B_0^4$
175	$A_0^1 B_0^2 C_0^1$ or $C_0^2 B_0^1$
180	$A_0^6$
195	$A_0^2 C_0^2$
202	$C_0^3$
205	$A_0^1 B_0^1 C_0^2$
210	$A_0^7$ or $B_0^5$
232	$A_0^1 C_0^3$

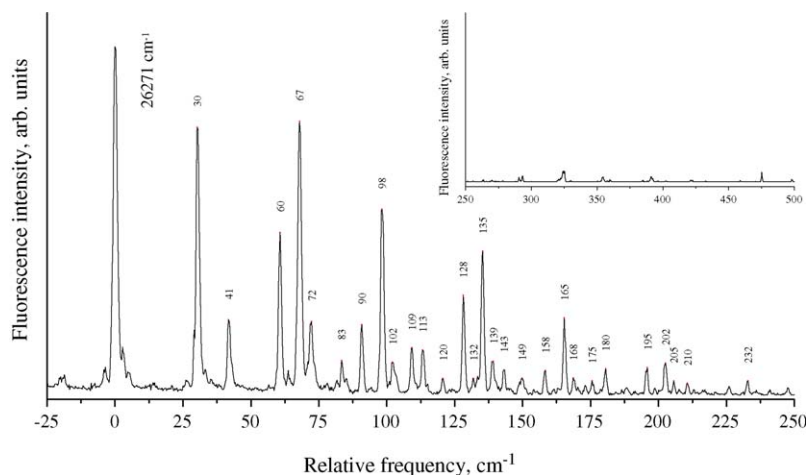


Fig. 8. The portion  $-25$  to  $250\text{ cm}^{-1}$  of the fluorescence excitation spectrum of the BPP molecule.

The most basic nitrogen atom in the neutral BPP molecule in the ground state is the pyrazole atom and thus it should be protonated as the first one. In the excited state, however, nitrogen atom in pyridine ring is the most basic. Thus, in the excited

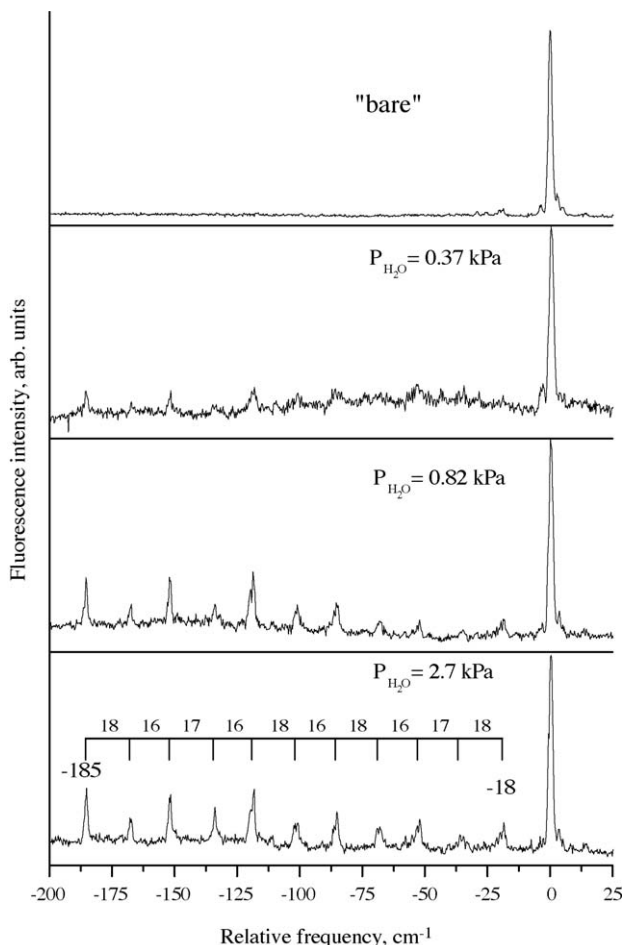


Fig. 9. Spectral changes of the fluorescence excitation spectrum of the BPP molecule with different vapor pressure of water.

molecule the protonation of this atom should be preferred. In the monocation protonated on pyrazole N atom, the second protonation should occur on the second pyrazole N atom in the ground state but in  $S_1$  excited state it should occur on pyridine N atom. On the other hand, the heat of formation of the cation protonated on the pyridine nitrogen atom calculated by AM1 method is 388 487 kcal/mol and for cation protonated on the pyrazole nitrogen is 402 093 kcal/mol. It shows that protonation of the pyridine nitrogen should be preferred in the ground state, contrary to the results of effective potential energies calculations. Thus, the question arises which approach is more valuable for the determination of the protonation sequence in heterocyclic compounds with several proton acceptor centers.

Table 2

Effective valence electron potentials,  $W_{2p}^N$  (eV), calculated for nitrogen atoms in heterocyclic system BPP and for cation  $H^+$  BPP, in which  $H^+$  is added to pyrazole ring

State	Neutral molecule			Molecule protonated on N2	
	$W_{2p}^{N2}$	$W_{2p}^{N8}$	$W_{2p}^{N6}$	$W_{2p}^{N8}$	$W_{2p}^{N6}$
$S_0$	-11.66	-11.87	-11.66	-15.51	-14.69
$S_1$	-11.86	-11.41	-11.87	-15.40	-16.64

Table 3

The effective valence electron potentials,  $W_{2p}^N$  (eV), calculated for nitrogen atoms in heterocyclic system DMA-DPPQ and for cation  $H^+$  DMA-DPPQ, in which  $H^+$  is added to  $N(CH_3)_2$

State	Neutral molecule		Molecule protonated on $N(CH_3)_2$	
	$W_{2p}^{N2}$	$W_{2p}^{N9}$	$W_{2p}^{N2}$	$W_{2p}^{N9}$
$S_0$	-11.56	-11.44	-13.90	-13.65
$S_1$	-11.68	-11.55	-13.60	-14.47

#### 4. Discussion

BPP has three types of nitrogen atoms in molecule and two kinds of potential protonation centers, one in the pyridine ring and two equivalent centers in the pyrazole subunits. The first protonation step is revealed in absorption and fluorescence spectra in acidified solutions in acetonitrile as the solvent. The absorption spectrum with the new first band peaking at about  $26\,300\text{ cm}^{-1}$  is ascribed to the absorption of the monocation. The quantum yield of the fluorescence of non-protonated molecule,  $F_{22\,600}$ , decreases with increasing concentration of the acid. The difference between the half values of the absorbance at  $24\,600\text{ cm}^{-1}$  and the quantum yield of the fluorescence  $F_{22\,600}$ , at about  $\log [HClO_4] = -3.5$  and  $-3.1$ , respectively may be caused by measurement inaccuracy, but also by some radiationless process deactivating BPP fluorescence and depending on the acid concentration. The new fluorescence band,  $F_{18\,000}$  appearing in appropriate acidity of the solution, reaches maximal value of its quantum yield at the acid concentration range in which  $F_{22\,600}$  disappears. We ascribe this fluorescence to the emission from the monocation as its fluorescence excitation spectrum corresponds to the absorption of the monocation (Fig. 6). The different excitation spectra of fluorescences  $F_{22\,600}$  and  $F_{18\,000}$  in solutions, in which both emitting states coexist, corroborate the statement that the fluorescence reflects the ground state protolytic reaction. It could mean that protolytic equilibrium in acetonitrilic solutions cannot be reached within the lifetime of the excited state.

According to highest value of effective valence potentials,  $W_{2p}^{N8}$ , the first protonation of BPP in acetonitrile in the ground state should occur on the one of pyrazolic atoms. Although the formation heat hint at the priority of pyridine nitrogen protonation, the insight into protolytic behaviour of DMA-DPPQ (Formula 2) [7] and the calculations of  $W_{2p}^N$  [5] confirm the validity of these indexes for the protonation sequence assignation in heterocyclic systems with several basic centers. The highest  $W_{2p}^{N9}$  value for non-protonated as well as protonated molecule on the amino group ( $N4'$ ) in the ground state (Table 3) hint at the first protonation of N9 (i.e. on pyridine). It should be mentioned that the atom N9 is more accessible in DMA-DPPQ for solvated proton than N8 atom in DMA-DMPP, due to steric hindrance of two phenyl groups in the last compound.

The amino group of DMA-DPPQ is protonated first in acetonitrilic solutions. The cation absorbs and intensively emits at shorter wavelength than the non-protonated molecule fluorescing from charge-transfer state (TICT) [7]. However, the

long wavelength new absorption band appears parallelly. The molecule excited in this band does not emit, like in the case of protonated *N,N*-dialkylaminopyridine and aminopyrimidine on nitrogen atom in aromatic ring [12]. This band can be ascribed to absorption of monocation with protonated atom N9. The further acidification leads to disappearance of this monocation. The second monocation, with protonated N4', forms a bication. According to potentials' calculations, the second atom protonated in this bication should be the pyrazolic one. The absorption spectra and fluorescence behaviour of bication closely resemble these of BPP and other bis-pirazolopyridine derivatives without 4'-aminogroup as well as the cation of DMA-DMPP [4]. Thus, we ascribe the absorption with maximum at  $24\,200\text{ cm}^{-1}$  and fluorescence  $F_{18\,000}$  of BPP to monocation with protonated pyrazolic N2 or N6 atom.

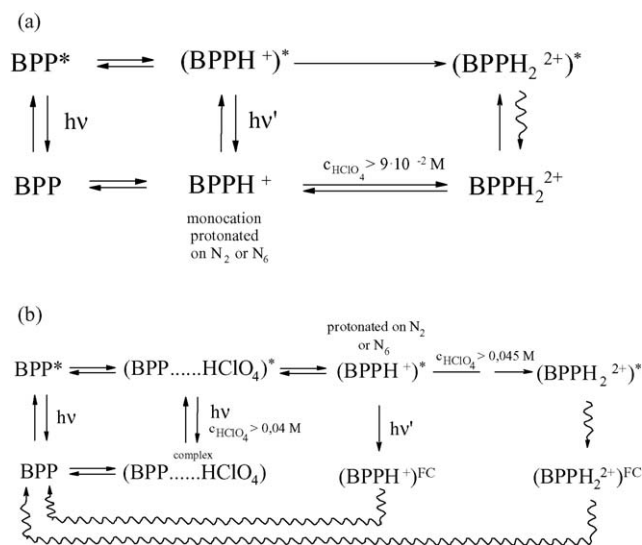
The  $\Delta pK_a \cong 6$  for the BPP was estimated from the Förster cycle. It suggests the larger basicity of the excited molecule than in the ground state and according to the decreased  $W_{2p}^{N8}$  values it hints at the preferential protonation of the pyridine N8 atom in the  $S_1$  excited state (see Table 2). We cannot check experimentally the validity of Spanget-Larsen's indexes in that case, because the fluorescence reflects the ground state equilibrium. This difficulty arises probably due to unequilibration of the system within the lifetime of the excited state.

The second protonation step is evidenced by changes of the absorption spectra in short wavelength range ( $30\,000\text{ cm}^{-1} < \tilde{\nu}$ ), Fig. 1c, and by the decrease of  $F_{18\,000}$  quantum yield, Fig. 3c. Thus, the bication has to be nonemissive.

In ethanolic solutions, the BPP reacts with the acid otherwise than in acetonitrile as solvents. The absorption changes are small, Fig. 2. The absorption characteristic for monocation (as in the case of acetonitrilic solutions) is absent. But the fluorescence changes resemble those in acetonitrile. They occur, however, at much higher acid concentration in ethanol than in acetonitrile. At high enough acid concentration ( $2.7 \times 10^{-2}\text{ M} < [\text{HClO}_4]$ ) the new fluorescence peaking at about  $18\,500\text{ cm}^{-1}$ ,  $F_{18\,500}$ , is distinctly observed, Fig. 5. The quasi-isoemissive point at  $21\,900\text{ cm}^{-1}$  appears, suggesting the equilibrium between the two forms. Practically, the same excitation spectra of both fluorescences,  $F_{22\,500}$  and  $F_{18\,500}$  hint at the adiabatic protonation in the excited state. The half value of  $F_{22\,500}$  emission at  $-\log [\text{HClO}_4] = 1.5$  does not coincide with that of  $F_{18\,500}$ , roughly estimated at  $-\log c = 0.7$ . It means that the non-protonated BPP has to be deactivated by some additional process before the isoemissive point appears. The small but noticeable change of absorption spectra may be caused by some kind of complexation of BPP, leading to the product with an emission similar to the non-complexed molecules, but with low quantum yield. At enough large  $\text{HClO}_4$  concentration, when all BPP molecules are complexed, the equilibrium complex-cation is established and the quasi-isoemissive point is observed.

At the highest acid concentrations under study, the isoemissive point disappears accompanied by the decrease of the long wavelength emission. It may suggest the creation of non-emissive bication.

The role of protic solvent in protonation of heterocyclic systems like BPP has to be further studied.



Scheme 1. The protonation equilibria in the ground and excited state for BPP in: (a) acetonitrile and (b) ethanol.

The complexation ability of BPP by water was investigated in molecular beams for the elucidation of the ability of formation of BPP–protic solvent complexes. In [13] various complexes of benzene and water were observed, many conformers could be formed at the same time. The clusters with geometry 1:1 exhibited long low frequency progression of  $17\text{ cm}^{-1}$  mode were found. The structure of benzene– $\text{H}_2\text{O}$  clusters was assigned in Ref. [13], as the  $\pi$ -hydrogen-bonded system. This assignment was done on the base of the energy stabilization of the 1:1 cluster. In the case of the BPP molecule, the benzene rings are practically separated from the rest of the molecule therefore one could expect that vibrational structure of BPP–water complexes will exhibit similar structure as in the case of benzene–water clusters. Moreover, the frequency of the progression in the BPP– $\text{H}_2\text{O}$  complex spectrum is in excellent agreement with results of Ref. [13]. This suggests that  $\text{H}_2\text{O}$  molecule is  $\pi$ -hydrogen-bonded to the one of BPP-benzene rings. Taking into account the lack of BPP protonation in the ground state in protic solvent (ethanol) it is worth to remarking the lack of either N2 (or N6) or N8 atom complexation by  $\text{H}_2\text{O}$  molecule in jet-experiment.

Basing on the above given data and considerations, the Scheme 1 can be proposed for the summarizing of the protolytic processes of BPP in the different non-aqueous solvents. The dashed lines correspond to some hypothetical reactions.

## 5. Conclusions

- (1) The protonation of BPP in non-aqueous solutions leads to the creation of the fluorescing monocation in the first step and non-emissive bication in the next step.
- (2) The first protonation occurs on the one of the pyrazolic nitrogen atom. The effective valence potential appear to be a valuable index for the determination of the protonation sequence in molecules with several protonation centers.
- (3) The character of the non-aqueous solvent plays an important role in the run of protolytic reactions. The BPP is effec-

tively protonated in the aprotic acetonitrile in the ground state and the fluorescence is practically not influenced by the reaction in the excited state. In protic solvent—ethanol, the protonation occurs in the excited state, but not in the ground state. However, some kind of BPP complexation by acid in ethanolic solutions in the ground state is suggested.

- (4) The H<sub>2</sub>O molecule forms  $\pi$ -hydrogen-bonded complex with one of the BPP-phenyl ring.

### Acknowledgements

The authors are indebted to Prof. Zbigniew R. Grabowski (Warsaw, Poland) for valuable remarks.

### References

- [1] Y.T. Tao, E. Balasubramaniam, A. Danel, P. Tomasik, Appl. Phys. Lett. 77 (2000) 933.
- [2] E. Balasubramaniam, Y.T. Tao, A. Danel, P. Tomasik, Chem. Mater. 12 (2000) 2788.
- [3] K.C. Joshi, K. Dubej, A. Dandia, Pharmazie 36 (1981) 336.
- [4] D. Piorun, A.B.J. Parusel, K. Rechthaler, K. Rotkiewicz, G. Köhler, J. Photochem. Photobiol. A Chem. 129 (1999) 33, and references therein.
- [5] D. Grabka, PhD Thesis, Świętokrzyska Academy Kielce, Institute of Chemistry, 2001.
- [6] A.B.J. Parusel, Private information.
- [7] A.B.J. Parusel, K. Rechthaler, D. Piorun, A. Danel, K. Khatchatryan, K. Rotkiewicz, G. Köhler, J. Fluoresc. 8 (1998) 375.
- [8] A. Brack, Liebigs Ann. Chem. 681 (1965) 105.
- [9] J. Spanget-Larsen, J. Phys. Org. Chem. 8 (1995) 496.
- [10] J. Spanget-Larsen, J. Chem. Soc. Perkin Trans. II (1985) 173.
- [11] J. Waluk, W. Rettig, J. Spanget-Larsen, J. Phys. Chem. 92 (1988) 6930.
- [12] Z.R. Grabowski, K. Rotkiewicz, W. Rettig, Chem. Rev. 103/10 (2003) 3899, and references therein.
- [13] A.J. Gotch, et al., Chem. Phys. Lett. 1 (1991) 178.